

Effect of focal spot size on in-band 13.5 nm extreme ultraviolet emission from laser-produced Sn plasma

Y. Tao, S. S. Harilal, M. S. Tillack, K. L. Sequoia, B. O'Shay, and F. Najmabadi

Department of Mechanical and Aerospace Engineering and the Center for Energy Research, University of California, San Diego, 9500 Gilman Drive, La Jolla, California 92093-0438

Received April 17, 2006; revised May 23, 2006; accepted June 12, 2006;
posted June 13, 2006 (Doc. ID 70008); published July 25, 2006

The effect of focal spot size on in-band 13.5 nm extreme ultraviolet (EUV) emission from laser-produced Sn plasmas was investigated for an EUV lithography light source. Almost constant in-band conversion efficiency from laser to 13.5 nm EUV light was noted with focal spot sizes from 60 to 500 μm . This effect may be explained by the opacity of Sn plasmas. Optical interferometry showed that the EUV emission must pass through a longer plasma with higher density when the focal spot is large, and strong reabsorption of EUV light was confirmed by a dip located at 13.5 nm in the spectrum. © 2006 Optical Society of America
OCIS codes: 350.5400, 300.6560, 120.3180.

Laser-produced Sn-based plasma has become one of the most promising candidates for an extreme ultraviolet (EUV) lithography source. What is believed to be the highest conversion efficiency (CE) to date, 3%, from laser to in-band (2% bandwidth) 13.5 nm EUV light has been demonstrated by use of a spherical Sn target uniformly irradiated by a 1.064 μm laser.¹ However, there is still a long way to go to satisfy the requirements of practical EUV lithography systems atomic number for high-volume production. Because of the high atomic number and the steep gradients in density and temperature, the physics of laser-produced Sn plasma has not been understood completely.

The properties of Sn plasma depend strongly on the parameters of the laser pulse. It has been shown that wavelength, pulse width, and focal spot size have large influences on 13.5 nm EUV light.²⁻⁴ Until now, for the effect of focal spot size, it has been widely accepted that to achieve high CE it is important to avoid energy loss due to lateral expansion by adopting a large focal spot.^{1,4,5} However, high CE has been reported by several groups using a very small focal spot. For example, Harilal *et al.*⁶ and Koay *et al.*⁷ demonstrated high CE using solid Sn targets with focal spot sizes of 60 and 35 μm , respectively. The reason for this may come from the opacity effect of laser-produced Sn plasmas. Previous works showed that laser-produced Sn plasma is optically thick to 13.5 nm EUV light.^{3,8} and that the plasma density profile plays a key role in optimizing a laser-produced plasma EUV laser source.⁹ When the focal spot size is comparable with the plasma scale length, there is a significant lateral expansion. In this case, the laser energy loss due to the lateral expansion should result in a lower CE than that of a larger focal spot; however, at the same time this lateral expansion could also reduce the normal thermal gradient, resulting in a smaller plasma scale length, which means less reabsorption of 13.5 nm EUV light induced by the plasma. In addition to lateral expansion, a small plasma volume with a small focal spot could also re-

duce the absorption. The final output of EUV light should be a result of the balance between the laser energy loss and reabsorption of 13.5 nm EUV light.

In this Letter, we present our investigations on the effect of focal spot size. Two lasers were employed in our experiments. One is a 7 ns Nd:YAG laser that can produce a 1.064 μm laser pulse with a pulse energy of 650 mJ at 10 Hz; the other is a picosecond (ps) frequency-doubled Nd:YAG laser (EKSPLA) that generates a 532 nm laser pulse with a pulse width of 130 ps. The nanosecond (ns) laser was used to generate the EUV plasma and is called the pump laser hereafter; the ps laser was employed as a probe beam. The two lasers are synchronized by a pulse delay generator (Stanford DG535), with a jitter less than 0.5 ns. The pump laser is focused onto the surface of the target placed in a vacuum chamber at normal incidence by a plano-convex lens with a focal length of 300 mm. A bulk Sn slab was used as the target. The chamber pressure can be pumped down to 10⁻⁶ Torr. The target is moved to maintain a fresh surface for each shot. The diameter (FWHM) of the focal spot is varied from 60 to 200 μm by moving the focusing lens.

The probe beam passes through the plasma parallel to the target surface and is relayed to an imager by an *f*/15 lens. A Normaski interferometer is inserted in front of the imager. The spatial resolution of the interferometer is less than 25 μm with a magnification of 7 \times . A multilayer interference filter is employed to block the plasma emission. The interferogram is recorded by an ICCD camera (Princeton, PI-MAX).

In-band CE was measured with a calibrated EUV energy monitor from Jenoptik that consists of a Zr filter, two near-normal-incident multilayer Mo/Si mirrors, and an x-ray photodiode. The CE is integrated over a 2 π solid angle. The spectrum of soft x-rays from laser-produced Sn plasmas was observed by a transmission grating spectrometer that consists of a 50 μm slit, a 10,000 line/mm transmission grating, and a backilluminated x-ray CCD camera (Roper).

The spectral resolution of the transmission grating spectrometer is better than 0.1 nm. Both the energy monitor and the spectrometer are installed in the plane of laser incidence at an angle of 45° with respect to the target normal.

The in-band CE of laser-produced Sn plasmas using focal spot sizes of 60 (blue triangle), 100 (black square), and $200\ \mu\text{m}$ (red circle) are plotted in Fig. 1. Regarding intensity dependence, it is noted that for a small spot size the optimum CE is achieved at a higher intensity than that of a larger spot size. This reveals that a smaller focal spot size requires a higher intensity to heat plasma to the optimum temperature for efficient 13.5 nm EUV emission. It is seen that for a $200\ \mu\text{m}$ spot CE depends weakly on laser intensities from 4×10^{10} to $1 \times 10^{11}\ \text{W}/\text{cm}^2$. Although the optimum CEs are achieved at different intensities for different spot sizes, they reach almost the same value if error bars are included. Okuno *et al.*¹⁰ obtained a similar CE $\sim 1.5\%$ when a $500\ \mu\text{m}$ focal spot was used.

This result conflicts with the well-accepted argument that for a small focal spot the laser energy loss induced by the significant lateral expansion should result in a lower CE than that of a larger focal spot. However, that argument does not include the effect of opacity,^{4,5} which plays a key role in the generation and transport of 13.5 nm EUV emission in laser-produced Sn-based plasmas.

To clarify the opacity effect of laser-produced Sn plasmas under different focal spot sizes, density profiles of laser-produced Sn plasma were observed with a temporally resolved interferometer. The plasma density profile is deduced from the interferograms by use of a mathematical treatment described in Ref. 9. The results for focal spot sizes of 100 (squares) and $200\ \mu\text{m}$ (circles) obtained at 2 ns after the peak of the pumping laser pulse in the line of laser incidence are shown in Fig. 2. The error comes from the irregularity of the phase shift profiles. The two solid curves in Fig. 2 represent the fit of the $100\ \mu\text{m}$ spot data by an exponential decay function $f(x) \propto \exp(-x/l_s)$ with scale lengths l_s of 20 and $86\ \mu\text{m}$. The dashed line shown in

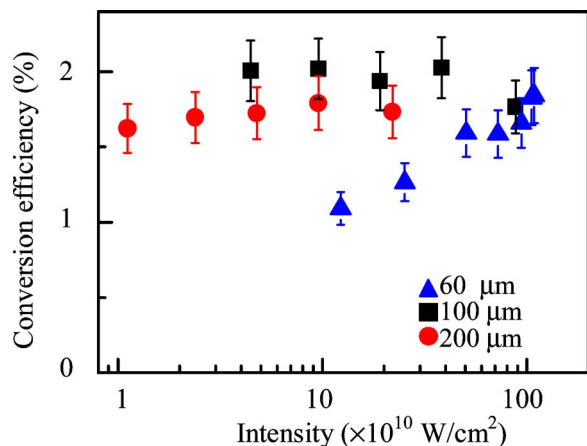


Fig. 1. (Color online) In-band conversion efficiency of laser-produced Sn plasmas using focal spot sizes of 60 (triangles), 100 (rectangles), and $200\ \mu\text{m}$ (solid dots) versus laser intensity.

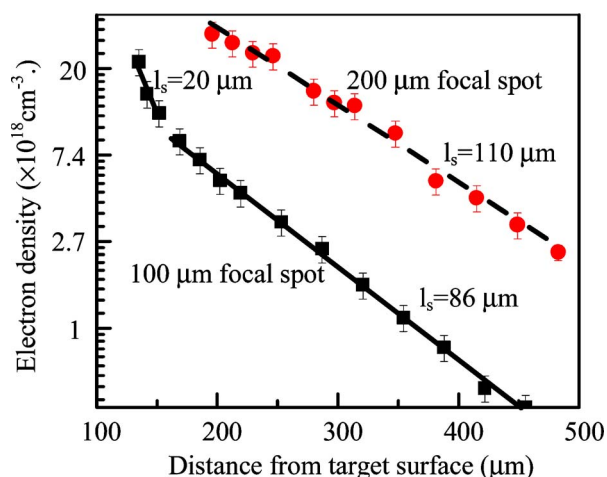


Fig. 2. (Color online) Density profiles of laser-produced Sn plasmas with focal spot sizes of $100\ \mu\text{m}$ (circles) and $200\ \mu\text{m}$ (squares) obtained at $2 \times 10^{11}\ \text{W}/\text{cm}^2$. The two solid curves represent the exponential decay fit of $100\ \mu\text{m}$ spot data with scale lengths of 20 and $86\ \mu\text{m}$, and the dashed line represents the fit of $200\ \mu\text{m}$ spot data with a scale length of $110\ \mu\text{m}$.

Fig. 2 is a fit of the $200\ \mu\text{m}$ spot data with a scale length of $110\ \mu\text{m}$. This confirms the assumption that the lateral expansion results in a shorter plasma scale length in the case of a small focal spot. It has been shown⁹ that the dominant emission region of 13.5 nm light is located around the plasma region with a density of several times $1 \times 10^{19}\ \text{cm}^{-3}$. To escape from the plasma, the EUV light must pass through the outer plasmas. In the case of a small focal spot, the EUV light need only transmit through the very short plasma with high density and a longer plasma with low density. But in the case of large spot size, the EUV light must pass through a longer plasma with higher density. So stronger reabsorption of EUV light should occur in the case of a large focal spot.

Typical spectra of laser-produced Sn plasmas with focal spot sizes of $60\ \mu\text{m}$ at intensities of 2×10^{11} and $8 \times 10^{11}\ \text{W}/\text{cm}^2$, $100\ \mu\text{m}$ at intensities of 2×10^{11} and $8 \times 10^{11}\ \text{W}/\text{cm}^2$, and $200\ \mu\text{m}$ at intensity of $2 \times 10^{11}\ \text{W}/\text{cm}^2$ are shown in Fig. 3. The spectra are normalized according to their corresponding laser energy. It is seen that when a $60\ \mu\text{m}$ focal spot is employed, spectra at different intensities look similar, except for the shift of the peak toward shorter wavelengths with increasing intensity. For a $100\ \mu\text{m}$ spot, when the intensity is lower than $2 \times 10^{11}\ \text{W}/\text{cm}^2$ the spectrum is similar to those in the case of a small spot; however, when the intensity is above $4 \times 10^{11}\ \text{W}/\text{cm}^2$ a dip centered at 13.5 nm starts to appear, and a significant dip can be seen in the spectrum obtained at $8 \times 10^{11}\ \text{W}/\text{cm}^2$, as shown in Fig. 3. For a $200\ \mu\text{m}$ focal spot, when the laser intensity is higher than $1 \times 10^{11}\ \text{W}/\text{cm}^2$, a spectral dip starts to appear. A significant dip is obvious at $2 \times 10^{11}\ \text{W}/\text{cm}^2$, as shown in Fig. 3. Okuno *et al.*¹⁰ also observed a spectral dip at $1 \times 10^{11}\ \text{W}/\text{cm}^2$ when a $500\ \mu\text{m}$ focal spot was employed. It is also seen in Fig. 3 that there is an additional peak in the long-

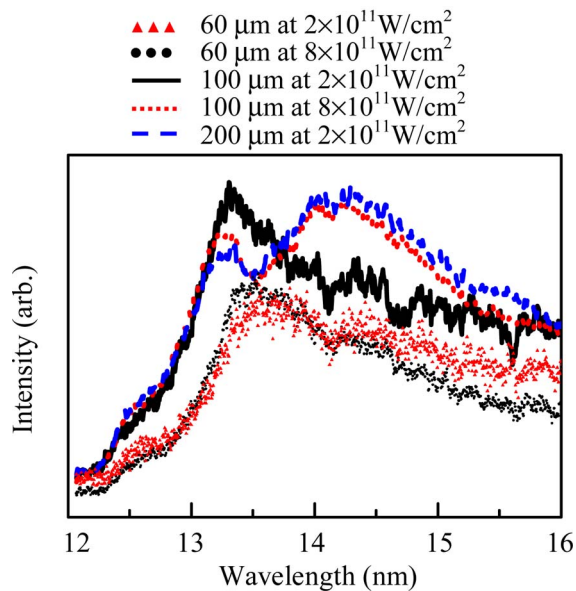


Fig. 3. (Color online) Spectra of laser-produced Sn plasmas using focal spot sizes of $60\ \mu\text{m}$ at intensities of 2×10^{11} (red triangles) and 8×10^{11} W/cm^2 (black dots), $100\ \mu\text{m}$ at intensities of 2×10^{11} (black solid curve) and 8×10^{11} W/cm^2 (red short-dashed curve), and $200\ \mu\text{m}$ at intensity of 2×10^{11} W/cm^2 (blue dashed curve).

wavelength side of the spectra when the spectral dip exists. This may come from reheating of plasma induced by reabsorbed short-wavelength radiation.

The spectral dip reveals strong reabsorption of $13.5\ \text{nm}$ EUV light induced by the EUV emitting plasma itself. For a small focal spot, significant lateral expansion can efficiently reduce the plasma scale length to avoid significant reabsorption even at high laser intensity. With increasing spot size, less lateral expansion occurs and lower intensity is required to reach the scale length to induce heavy reabsorption. This is confirmed by previous research carried out using a $220\ \mu\text{m}$ focal spot, which pointed out that when the laser intensity is above 1×10^{11} W/cm^2 a long plasma scale length could result in heavy reabsorption and lower CE.¹¹

These results clearly show the following: (1) For a small spot, significant lateral expansion wastes laser energy and less $13.5\ \text{nm}$ EUV light is generated, but at the same time a short plasma scale length as a result of lateral expansion and small plasma volume reduces reabsorption of the $13.5\ \text{nm}$ light so that more $13.5\ \text{nm}$ EUV light can escape from the plasma. (2) For a large spot size, more EUV light can be generated due to high hydrodynamic coupling efficiency, but the longer plasma scale length results in stronger reabsorption so that less $13.5\ \text{nm}$ light can escape from the plasma. The final output of $13.5\ \text{nm}$ EUV light is determined by the balance of the laser energy loss and the reabsorption of the EUV light. So almost constant CEs are observed for a wide range of focal spot sizes.

To further understand the physics related to the effect of focal spot size, two-dimensional hydrodynamic simulation including radiation transport is required.

The design of a practical EUV laser system can benefit from this research. As mentioned above, a Sn plasma with a large spot size is not sensitive to fluctuation of laser intensity. By adopting a large focal spot size, the instability of a practical high-repetition-rate laser used in a EUV laser source can be mitigated. Then the stability of the EUV laser source can be improved. To avoid heavy reabsorption of $13.5\ \text{nm}$ light in a large spot size plasma as shown in Fig. 3, low intensity is required. It is also seen in Fig. 1 that high CE is achieved at low intensity for a large spot size. Furthermore, it is easier to get a high plug efficiency and a high average power for a low-intensity laser than for a high intensity laser, and low intensity is helpful to reduce the kinetic energy and the amount of debris generated from the plasma.¹² So the combination of a large spot size and low intensity may be advantageous in making an efficient, clean, and stable laser-produced Sn plasma EUV laser source.

Y. Tao's e-mail address is yetao@ucsd.edu.

References

1. Y. Shimada, H. Nishimura, M. Nakai, K. Hashimoto, M. Yamaura, Y. Tao, K. Shigemori, T. Okuno, K. Nishihara, T. Kawamura, A. Sunahara, T. Nishikawa, A. Sasaki, K. Nagai, T. Norimatsu, S. Fujioka, S. Uchida, N. Miyanaga, Y. Izawa, and C. Yamanaka, *Appl. Phys. Lett.* **86**, 051501 (2005).
2. M. Yamaura, S. Uchida, A. Sunahara, Y. Shimada, H. Nishimura, S. Fujioka, T. Okuno, K. Hashimoto, K. Nagai, T. Norimatsu, K. Nishihara, N. Miyanga, Y. Izawa, and C. Yamanaka, *Appl. Phys. Lett.* **86**, 181107 (2005).
3. S. Fujioka, H. Nishimura, K. Nishihara, A. Sasaki, A. Sunahara, T. Okuno, N. Ueda, T. Ando, Y. Tao, Y. Shimada, K. Hashimoto, M. Yamaura, K. Shigemori, M. Nakai, K. Nagai, T. Norimatsu, T. Nishikawa, N. Miyanaga, Y. Izawa, and K. Mima, *Phys. Rev. Lett.* **95**, 235004 (2005).
4. R. C. Spitzer, T. J. Orzechowski, D. W. Phillion, R. L. Kauffman, and C. Cerjan, *J. Appl. Phys.* **79**, 2251 (1996).
5. C. Cerjan, *Appl. Opt.* **32**, 6911 (1993).
6. S. S. Harilal, B. O'Shay, M. S. Tillack, Y. Tao, R. Paguio, A. Nikroo, and C. A. Back, *J. Phys. D* **39**, 484 (2006).
7. C.-S. Koay, S. George, K. Takenoshita, R. Bernath, E. Fujiwara, M. Richardson, and V. Bakshi, in *Proc. SPIE* **5751**, 279 (2005).
8. T. Aota and T. Tomie, *Phys. Rev. Lett.* **94**, 015004 (2005).
9. Y. Tao, H. Nishimura, S. Fujioka, A. Sunahara, M. Nakai, T. Okuno, N. Ueda, K. Nishihara, N. Miyanaga, and Y. Izawa, *Appl. Phys. Lett.* **86**, 201501 (2005).
10. T. Okuno, S. Fujioka, H. Nishimura, Y. Tao, K. Nagai, Q. Gu, N. Ueda, T. Ando, K. Nishihara, T. Norimatsu, N. Miyanaga, Y. Izawa, and K. Mima, *Appl. Phys. Lett.* **88**, 161501 (2006).
11. Y. Tao, H. Nishimura, T. Okuno, S. Fujioka, N. Ueda, M. Nakai, K. Nagai, T. Norimatsu, N. Miyanaga, K. Nishihara, and Y. Izawa, *Appl. Phys. Lett.* **87**, 241502 (2005).
12. S. Bollanti, F. Bonfigli, E. Burattini, P. Di Lazzaro, F. Flora, A. Grilli, T. Letardi, N. Lisi, A. Marinai, L. Mezi, D. Murra, and C. Zheng, *Appl. Phys. B* **76**, 277 (2003).